JHR 98: 757–778 (2025)
doi: 10.3897/jhr.98.158760
https://jhr.pensoft.net

RESEARCH ARTICLE

JOURNAL OF Hymenoptera RESEARCH
A peer-reviewed open-access journal
The International Society of Hymenopterists

First report of the genus *Heinrichiellus* Tereshkin, 2009 (Hymenoptera, Ichneumonidae) from the Oriental region with the description of three new species

A. P. Ranjith[1,2], Gavin R. Broad[3], Bernardo F. Santos[4], Buntika A. Butcher[1]

1 *Integrative Insect Ecology Research Unit, Department of Biology, Faculty of Science, Chulalongkorn University, Bangkok, Thailand* **2** *Kālinga Foundation, Agumbe, Karnataka, India* **3** *The Natural History Museum, Cromwell Road, London SW7 5BD, UK* **4** *Center for Integrative Biodiversity Discovery, Museum für Naturkunde, Invalidenstraße 43, 10115 Berlin, Germany*

Corresponding author: Buntika A. Butcher (buntika.a@chula.ac.th)

Academic editor: Tamara Spasojevic | Received 13 May 2025 | Accepted 11 August 2025 | Published 28 August 2025

https://zoobank.org/C198839C-397F-466C-94CC-F1844CFB5F36

Citation: Ranjith AP, Broad GR, Santos BF, Butcher BA (2025) First report of the genus *Heinrichiellus* Tereshkin, 2009 (Hymenoptera, Ichneumonidae) from the Oriental region with the description of three new species. Journal of Hymenoptera Research 98: 757–778. https://doi.org/10.3897/jhr.98.158760

Abstract

The ichneumonine genus *Heinrichiellus* Tereshkin is reported for the first time from the Oriental region. Three new species (*Heinrichiellus natgeo* Ranjith & Broad, **sp. nov.**, *Heinrichiellus vedani* Ranjith, **sp. nov.** from India and *Heinrichiellus brevispinus* Ranjith & Broad, **sp. nov.** from Thailand) are described. A revised generic diagnosis and an identification key to the known species are provided. Additionally, the systematic placement of the genus within the subfamily Ichneumoninae is proposed for the first time based on data from four genes.

Keywords

Ichneumoninae, molecular phylogeny, new species, taxonomic key, taxonomic placement

Introduction

Heinrichiellus Tereshkin 2009 is a small genus of Ichneumoninae previously comprising two species in the Eastern Palaearctic region: *Heinrichiellus hildegardae* (Tereshkin 1996) from Russia and *Heinrichiellus nambui* Kikuchi & Konishi, 2015 from Japan. The main diagnostic features of this distinctive genus are: antennal cavity absent;

Copyright *A. P. Ranjith et al.* This is an open access article distributed under the terms of the Creative Commons Attribution License (CC BY 4.0), which permits unrestricted use, distribution, and reproduction in any medium, provided the original author and source are credited.

maxillary palp extremely long and thin; mesopleuron with a sharp sternaulus; very long and slender legs; and a long but not flattened metasomal petiole (Tereshkin 1996, 2009; Kikuchi and Konishi 2015). The unique set of morphological characters which render *Heinrichiellus* distinct also make its tribal placement complicated. Tereshkin (1996, 2009) placed *Heinrichiellus* in the tribe Platylabini based on the convex clypeus, narrow mandibles, highly elevated scutellum and amblypygous metasoma. However, other distinctive characters (particularly the absence of the antennal cavity, long and thin maxillary palps, large fore wing areolet and a long sternaulus) are not found in typical platylabines. The long, complete sternaulus is very unusual in Ichneumoninae and is more typical of the subfamilies Cryptinae and Phygadeuontinae (Kikuchi and Konishi 2015). The higher level placement of *Heinrichiellus* had not previously been tested using molecular data.

The most recent and comprehensive phylogenetic analysis of Ichneumoninae (Santos et al. 2021) showed almost no support for previous tribal classification schemes, with most characters traditionally supporting higher-level taxa found to be examples of rampant morphological convergence. The main exceptions were that the Phaeogenini and Platylabini were largely monophyletic, with the latter including *Cotiheresiarches* Telenga, 1929 and *Probolus* Wesmael, 1845, traditionally included in other tribes.

In the present study we report three new species of *Heinrichiellus* from the Oriental region, from India and Thailand. A revised generic diagnosis and identification key are provided for the known species of *Heinrichiellus* along with the first assessment of the phylogenetic placement of the genus based on molecular data.

Materials and methods

Indian specimens were collected by yellow pan trap from Yingku, Arunachal Pradesh, Biligiri Rangaswamy Temple Tiger Reserve, Karnataka, and the Thai specimens were collected by Malaise trap from Doi Chiang Dao National Park, Chiang Mai as part of the "Thailand Inventory Group for Entomological Research" (TIGER) project (grant #DEB-0542864). Specimens were photographed with a Keyence VHX-6000 digital microscope (India) and a Leica M205 C stereomicroscope with a DMC5400 Camera (Thailand) and stacked in LASX.

Morphological terminology follows Broad et al. (2018) and cuticular sculpture follows Harris (1979).

List of repositories

ZSIK National Zoological Collections of the Zoological Survey of India, Western Ghats Regional Centre, Kozhikode, Kerala, India

QSBG Queen Sirikit Botanic Garden, Chiang Mai, Thailand

Sequencing and phylogenetic analysis

Sequences for three molecular markers (cytochrome oxidase I, 16S rRNA and 28S rRNA) were obtained from the new Indian species, *H. natgeo*, based on standard protocols as described in Hebert et al. (2003, 2004), Park et al. (2010), Magnacca and Brown (2010), Belshaw and Quicke (1997) and Quicke et al. (2020, 2023). Polymerase chain reaction (PCR), amplification and DNA sequencing were performed following standard protocols for DNA extraction, PCR and sequencing (Hajibabaei et al. 2005; Ivanova et al. 2006; de Waard et al. 2008). The newly generated sequences were submitted to Genbank with the following accession numbers; COI PQ858774, 16S PQ873015, 28S PQ873014.

In order to place *Heinrichiellus* in phylogenetic context, we used a "hybrid dataset" approach (Santos and Brady 2024) combining the newly generated Sanger sequencing data with the UCE dataset of Santos et al. (2021). To that end, we used the script assembly_match_contigs_to_ barcodes from the Phyluce v1.5 pipeline (Faircloth 2016) to bioinformatically extract sequences of the three loci available for *Heinrichiellus* from the assemblies generated by the raw sequencing data from the Santos et al. (2021) dataset. As a template for the script, we used ~20 sequences available for ichneumonine, phygadeuontine and cryptine taxa from Santos (2017).

Captured sequences for each locus (Table 1) were aligned using MAFFT (Katoh et al. 2002) under the same parameters as in Santos (2017). A rapid Neighbour-Joining tree produced in Geneious (Biomatters) was used to identify abnormally long branches which usually corresponded to contaminants. Sequences shorter than 200 bp, or representing contaminants, or containing stop codons (for COI) were removed and the samples were re-aligned once more prior to phylogenetic analyses, resulting in a three-gene matrix with 298 terminal taxa and 2,682 base pairs. This was combined with the original UCE data from Santos et al. (2021) assembled at 50% completeness for a hybrid analysis (Suppl. material 1).

As the goal of this analysis was simply to place *Heinrichiellus* in a phylogenetic context within the ichneumoniformes group of subfamilies, the dataset was analysed with the topology constrained to conform to the results of the previous UCE analysis of Santos (2021). Maximum likelihood analyses were conducted with IQTREE v1.6.12 (Nguyen et al. 2015), with topology constraint implemented via the -g option; 10,000 rounds of ultra-fast bootstrapping (Hoang et al. 2018) and an implementation of the SH- like approximate likelihood ratio test (SH-a LRT; Guindon et al. 2010) to assess clade support; and using ModelFinder (Kalyaanamoorthy et al. 2017) to choose the best model for each partition via the option -MFP. Both UCE and ribosomal data were partitioned by loci while COI data were partitioned by codon position. Analyses were run with the safe numerical mode (option - safe) to avoid numerical underflow that can result from large datasets. The tree was rooted with the xoridine *Odontocolon albotibiale* (Bradley), as in the original analyses of Santos et al. (2021).

Table 1. Success metrics for the capture of Sanger loci as bycatch from the UCE sequencing raw reads.

Locus	# recovered sequences	Mean length (bp)
16S rRNA	257	428.6
28S rRNA	273	739.3
COI	266	516.9

Results and discussion

Phylogeny

Maximum likelihood analyses recovered *Heinrichiellus* firmly as part of Ichneumoninae, but not in Platylabini as hypothesized by Tereshkin (1996); instead, the genus was recovered inside the Ichneumonini, nested in a polytomy with *Plagiotrypes concinnus* (Say) and *Imeria seyrigi* (Heinrich) (Fig. 1; Suppl. material 2). It is likely that the lack of resolution among the three species in this subclade derives simply from low volume of data (only the three Sanger loci) available to resolve this relationship rather than a true "hard polytomy" (sensu Purvis and Garland 1993). While bootstrap support was low for the exact sister group of *Heinrichiellus*, its placement within Ichneumonini was maximally supported. *Heinrichiellus* displays a number of morphological similarities with *Plagiotrypes* that could be interpreted as synapomorphies for the two genera: the scutellum has strong, complete lateral carinae; long, pointed apophyses on the propodeum; female hypygium large; and male gonostyle apically strongly narrowed. *Plagiotrypes* differs from *Heinrichiellus* by the unidentate mandible, narrowly pentagonal areolet, short sternaulus, slightly concave frons, and the modified end to the female metasoma, in which the

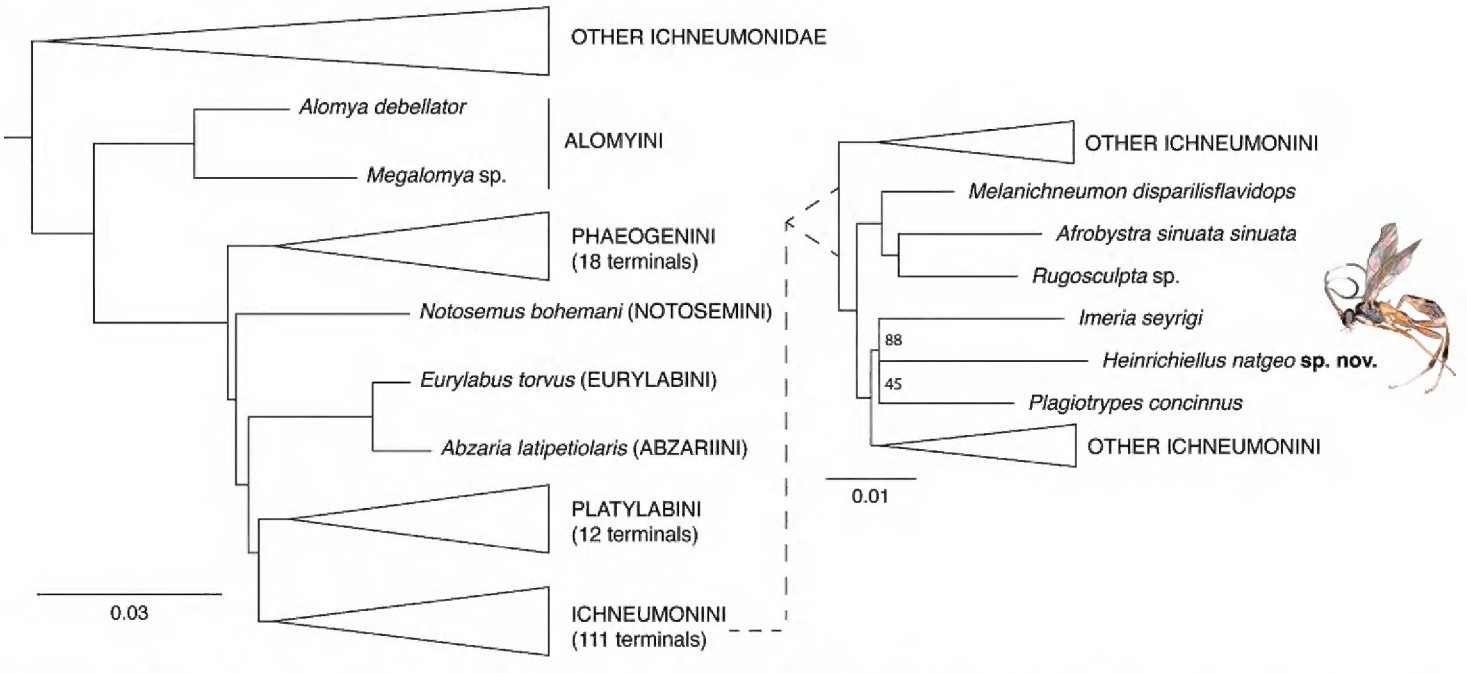

Figure 1. Section of maximum-likelihood tree generated by combining the UCE dataset from Santos et al. (2021) with data from the COI, 16S and 28S genes to place *Heinrichiellus* into phylogenetic context. Left side image shows a schematic view of the higher level relationships, with the immediate vicinity of *Heinrichiellus* in the tree depicted on the right side. Bootstrap support was maximal except where indicated in the tree by node numbers.

apex is dorso-ventrally flattened. *Imeria* are not so morphologically similar but, interestingly, have very strong scutellar carinae and a flat or convex frons, like *Heinrichiellus*. The antenna is long and slender in all three genera and the first tergite is somewhat similar in structure, with the postpetiole poorly differentiated and the petiole quite stout.

Our results highlight the extent of morphological convergence in Ichneumoninae. Tereshkin (2009) followed previous authors in defining Platylabini on the basis of a convex clypeus, flattened petiole of the first metasomal tergite and an amblypygous metasoma (i.e., a large hypopygium). Other trends are also common to large subsets of Platylabini, such as a strongly elevated scutellum. However, while many Platylabini do have a distinctive appearance, and many northern temperate genera, at least, are parasitoids of Geometridae or Drepanidae, various genera treated by Tereshkin (2009) and others as platylabines are aberrant in lacking the flattened petiole or in having a flatter clypeus. Conversely, some genera of Ichneumonini can have a flattened petiole, a fairly convex clypeus or be amblypygous. Santos et al. (2021) found that *Abzaria* Cameron and *Levansa* Townes do not belong in Platylabini but, conversely *Cotiheresiarches* and *Probolus* do belong in the tribe. *Abzaria* bears very little resemblance to Platylabini so it is unclear why Tereshkin (2009) classified it there. However, Tereshkin (2009) singled out *Heinrichiellus* as the only genus of Platylabini which was difficult to classify in a tribe and, when describing the genus (as *Heinrichia*) (Tereshkin 2009) had suggested that a new tribe might be warranted. In reality, the morphology of the clypeus is very variable within Ichneumonini and the 'amblypygous condition' has evolved repeatedly. Interpreting the ambiguous morphology is made a lot easier with molecular data, with long apophyses and a strongly elevated, carinate scutellum being apomorphies of a group of Ichneumonini genera as well, presumably, as some Platylabini.

Taxonomy

Genus *Heinrichiellus* Tereshkin, 2009

Heinrichia Tereshkin, 1996: 86 (unavailable name). Preoccupied by *Heinrichia* Stresemann, 1931 (Aves, Passeriformes). Type species: *Heinrichia hildegardae* Tereshkin, by monotypy.

Heinrichiella Tereshkin, 2000: 232 (unavailable name). New name for *Heinrichia* Tereshkin, 1996. Preoccupied by *Heinrichiella* Hedwig, 1949 (Hymenoptera, Ichneumonidae).

Heinrichiellus Tereshkin, 2009: 1535. New name for *Heinrichiella* Tereshkin, 2000.

Heinrichiola Koçak & Kemal, 2009: 1. New name for *Heinrichiella* Tereshkin, 2000.

Diagnosis. Head often longer than wide in anterior view (Figs 2B, 5B). Antennal cavity absent (Figs 2B, E, 5B). Clypeus convex, apical margin often straight, sometimes slightly concave medially (Figs 3A, 5B). Antenna long and slender (Figs 2A, 5A). Inner margins of eyes parallel (Figs 2B, 5B). Occipital carina joining hypostomal carina above base of mandible (Figs 2F, 5D). Maxillary palps long (Figs 3B, 5D). Notauli reaching middle of

mesoscutum (Figs 3D, 5F). Scuto-scutellar sulcus smooth without crenulations (Figs 3D, 5F). Scutellum highly elevated above metanotum (Figs 3C, 5E) with complete lateral carina extending to posterior end (Figs 3D, 5F). Epicnemial carina complete (Figs 3C, 5E). Subtegular ridge sharp (Figs 3C, 5E). Sternaulus sharp, almost reaching base of mid coxa (Figs 3C, 5E). Posterior transverse carina of mesosternum absent (Figs 3D, 5F). Hind margin of metanotum with a triangular projection on each side of metanotum (Figs 3E, F, 5F, 6A). Propodeum with apophyses, usually long (Figs 5E, 6A, C), rarely short (in *Heinrichiellus brevispinus* sp. nov.) (Fig. 3C, E, F). Area basalis mostly defined by carinae (Fig. 6A), rarely not (in *Heinrichiellus brevispinus* sp. nov.) (Fig. 3E). Area superomedia pentagonal or hexagonal (Figs 3E, 6A). Propodeal spiracle 1.4–3.0 × as long as wide (Figs 3E, F, 6A). Fore wing with large pentagonal areolet, often narrowing anteriorly (Fig. 4E) or 2*rs-m* and 3*rs-m* subparallel (in *Heinrichiellus natgeo* sp. nov.) (Fig. 6E). All legs longer than fore wing (Figs 2A, 5A). Tarsal claws simple (Fig. 4D). Petiole long, rounded in cross-section (Figs 4A, B, 6B). Gastrocoelus in the form of a longitudinal furrow with thyridium in the form of a small circle, metasoma amblypygous (Figs 2A, 4A–C, 5A, 6B–D). Ovipositor short (Figs 4A, 6B). Ovipositor sheath setose (Figs 4A, 6B).

Distribution. Eastern Palaearctic (Russia and Japan) and Oriental (India and Thailand) regions.

Hosts. Unknown.

Key to *Heinrichiellus* species

1 Area superomedia wider than long; area basalis not defined by carinae; frons extensively yellow medially; dorsal length of eye 3.7 × as long as temple (Fig. 2C) **2**

– Area superomedia often longer than wide; area basalis defined by carinae; frons black or brown medially; dorsal length of eye 1.2–1.7 × as long as temple (Fig. 5C) **3**

2 Area petiolaris not defined laterally by carinae; juxtacoxal carina incomplete, absent posteriorly; mesopleuron mostly punctate posteriorly; metasomal tergites 3 & 4 mostly yellowish [Thailand] ..... ***Heinrichiellus brevispinus* Ranjith & Broad, sp. nov.**

– Area petiolaris distinctly defined laterally by carinae; juxtacoxal carina complete, distinct posteriorly; mesopleuron mostly obliquely strigose posteriorly; metasomal tergites 3 & 4 entirely brownish black [India] ..... ***Heinrichiellus vedani* Ranjith, sp. nov.**

3 Head wider than long (Fig. 5B); propodeal spiracle 1.4 × as long as wide; clypeus slightly concave antero-medially (Fig. 5B); area petiolaris transversely strigose (Fig. 6A); fore wing areolet not narrowing anteriorly (Fig. 6E) [India] ..... ***Heinrichiellus natgeo* Ranjith & Broad, sp. nov.**

– Head longer than or as long as wide; propodeal spiracle 2.5–3.0 × as long as wide; clypeus straight antero-medially; area petiolaris variable; fore wing areolet strongly narrowing anteriorly **4**

4 Juxtacoxal carina complete; area superomedia parallel-sided; mesopleuron microsculptured; fore wing areolet asymmetrical [Russia] ..... ***Heinrichiellus hildegardae*** **(Tereshkin)**

– Juxtacoxal carina incomplete, distinct basally; area superomedia wider posteriorly; mesopleuron obliquely strigose; fore wing areolet symmetrical [Japan] ..... ***Heinrichiellus nambui*** **Kikuchi & Konishi**

Description of new species

Heinrichiellus brevispinus **Ranjith & Broad, sp. nov.**
https://zoobank.org/EF47DD0E-542D-46DE-B90D-D78D9440BEA6

Material examined. ***Holotype*****:** • female, Thailand: Chiang Mai, Doi Chiang Dao National Park, 14–21.x.2007, Malaise trap, coll. Songtran & Apaichat, T3172 (QSBG). ***Paratype*****:** • 1 male with same data as holotype (QSBG).

Holotype. ♀, body length 11.7 mm, fore wing length 8.6 mm.

Description of female. ***Head.*** Head 1.4 × as wide as high in anterior view, 2.0 × as wide as long in dorsal view, coriaceous except area between polished antennal sockets (Fig. 2B, E); ocellar-ocular length (OOL)/postero-ocellar length (POL) = 0.9. Frons slightly convex above each antennal socket (Fig. 2C); frons granulate with small and distinct tubercle between antennal sockets (Fig. 2B, C, E); antennal sockets large and protruding anteriorly in dorsal view (Fig. 2C); face 1.2 × as wide as high, granulate (Fig. 2B); inner margins of compound eyes parallel (Fig. 2B); clypeus strongly convex and transverse, 1.9 × as wide as high, with straight apical margin (Fig. 3A); anterior tentorial pits large (Fig. 3A); labrum very wide, 0.6 × as wide as clypeus, with straight apical margin, protruding from under clypeus. Mandible slender, 2.2 × as long as wide at base, gradually narrowed from base to apex, with indistinct lower tooth (Fig. 3A). Malar space granulate, 1.1 × as wide as base of mandible (Fig. 2D, F). Occipital carina complete, joining hypostomal carina above base of mandible (Fig. 2F); dorso-median part of occipital carina evenly arched (Fig. 2C). Maxillary palp long, reaching epicnemial carina (Fig. 3B); fifth segment 4.5 × as long as mandible base. Dorsal length of eye 3.7 × as long as temple. Antenna with 36 antennomeres. Flagellum bristle-shaped, very long and slender (Fig. 2A); apical flagellomere conical; first flagellomere 6.7 × as long as apical width and 1.5 × as long as second flagellomere.

Mesosoma. Mesosoma 1.6 × as long as high. Collar of pronotum long (Fig. 3C, D). Pronotum smooth, strigose postero-laterally (Fig. 3C). Mesoscutum strongly convex (Fig. 3C) with notaulus reaching middle of mesoscutum (Fig. 3D); mesoscutum granulate with scattered punctures except longitudinally strigose notaular region (Fig. 3D). Epicnemial carina complete (Fig. 3C); subtegular ridge sharp (Fig. 3C); impression below speculum weak (Fig. 3C); sternaulus distinct, crenulate, sharp, almost reaching base of mid coxa (Fig. 3C); posterior transverse carina of mesosternum absent; surface of mesopleuron obliquely strigose medially, smooth anteriorly, posteriorly punctate, speculum slightly polished (Fig. 3C). Scutellum highly elevated above metanotum (Fig. 3C), with

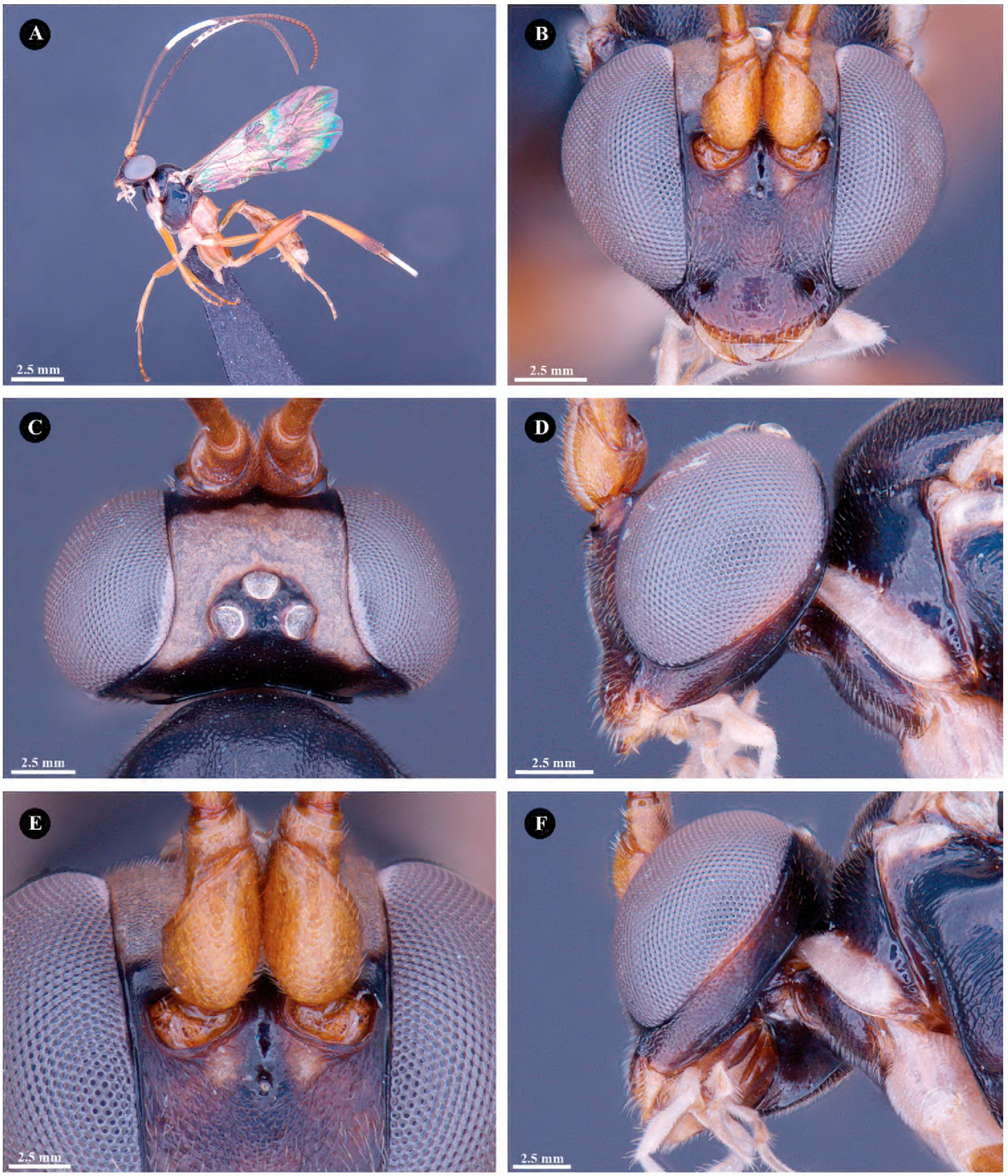

Figure 2. *Heinrichiellus brevispinus* Ranjith & Broad, sp. nov., holotype, female **A** habitus, lateral view **B** head, anterior view **C** head, dorsal view **D** head, lateral view **E** antennal torulus **F** head, ventro-lateral view.

lateral carina reaching apex and dorsal surface almost flat (Fig. 3D); hind margin of metanotum with a triangular projection on each side of metanotum (Fig. 3E, F). Juxtacoxal carina distinct anteriorly, incomplete (Fig. 3C). Propodeum in profile with area basalis flat and unevenly slanted from base of area superomedia (Fig. 3C), area basalis not defined by carinae (Fig. 3E); regular carinae of propodeum complete (Fig. 3E); area superomedia hexagonal, 0.8 × as long as wide (Fig. 3E); apex of area dentipara with strongly developed,

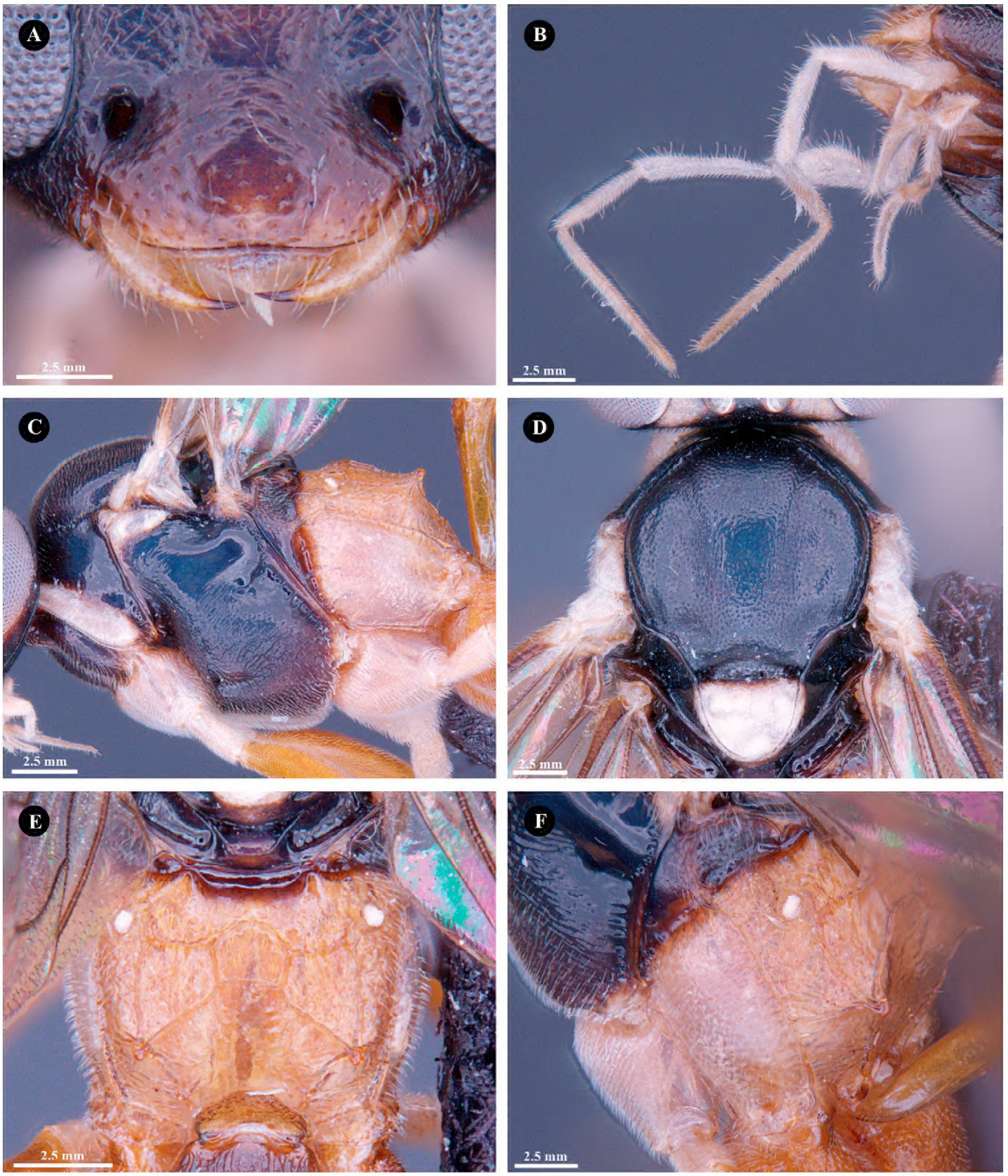

Figure 3. *Heinrichiellus brevispinus* Ranjith & Broad, sp. nov., holotype, female **A** clypeus and mandible, anterior view **B** maxillary and labial palps **C** mesosoma, lateral view **D** mesosoma, dorsal view **E** propodeum, dorsal view **F** propodeum, dorso-lateral view.

short and sharp apophysis, almost perpendicular to surface of propodeum, almost straight (Fig. 3E); surface of propodeum unevenly corrugated (Fig. 3E); area petiolaris indistinct laterally, smooth (Fig. 3E). Propodeal spiracle 1.4 × as long as wide (Fig. 3F).

Legs. Legs very slender and long (Fig. 2A); all legs longer than fore wing. Hind femur and tibia 4.0, 7.1 × as long as maximum width respectively; ratio of length of tibiae fore:mid:hind = 1.0:1.1:1.8.

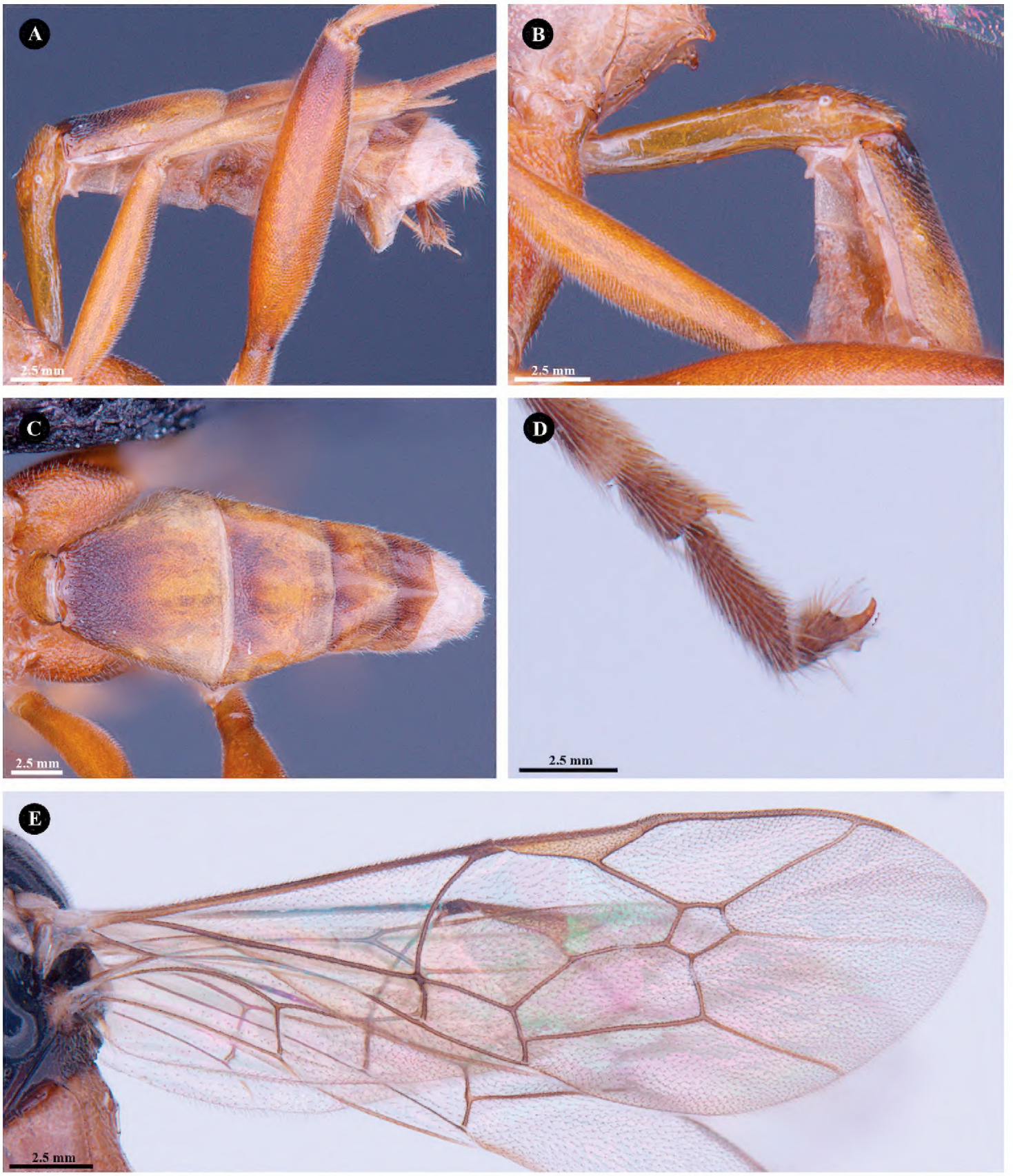

Figure 4. *Heinrichiellus brevispinus* Ranjith & Broad, sp. nov., holotype, female **A** metasoma, lateral view **B** first metasomal tergite, lateral view **C** metasomal tergites 2–6, dorsal view **D** tarsal claw **E** wings.

Wings. Fore wing 5.9 mm long; areolet 1.3 × as wide as long, 1.7 × as high as 3rs-m, 0.9 × as high as 2m-cu, pentagonal and narrowing anteriorly (Fig. 4E); 1cu-a opposite M&RS (Fig. 4E); ramulus very short (Fig. 4E). Hind wing with cu-a one-fourth as long as first abscissa of CU (Fig. 4E).

Metasoma. Metasoma mostly coriaceous (Fig. 4A–C). First tergite in profile almost straight, slightly bent downward at base of postpetiole; smooth anteriorly, irregularly

sculptured between latero-median carinae (Fig. 4A, B); in dorsal view 5.1 × as long as wide at base; petiole very long, rounded in cross-section, of approximately equal width and height; in dorsal view petiole slightly broadened posteriorly; latero-median carina present only on anterior portion of postpetiole (Fig. 4A, B). Second tergite in dorsal view 2.1 × as long as wide anteriorly, distinctly minutely punctate, longitudinally strigose anteriorly (Fig. 4C). Gastrocoelus slightly impressed, in form of longitudinal groove (Fig. 4C). Thyridium oval, distant from anterior of second tergite by 0.2 × its length (Fig. 4C). Tergites 3–6 with laterotergites separated by distinct crease (Fig. 4A). Sternites 2–5 laterally sclerotized and middle part not sclerotized (Fig. 4A). Hypopygium with apical margin rounded and longitudinally folded in middle. Ovipositor sheath with apex pointed, protruding beyond apex of metasoma (Fig. 4A).

Colour. Body mostly yellow except for following: flagellomeres 2–7, 15–36, face, clypeus, frons anteriorly, ocellar area, vertex and occiput, temple, pronotum except laterally, propleuron, mesoscutum, metanotum, mesopleuron, wing venation dark brown to black, mid tarsus, second metasomal tergite anterior half, third and fourth metasomal tergites anteriorly, fifth metasomal tergite yellowish, ovipositor sheath brown,

Male. Same as female.

Distribution. Oriental region (Thailand).

Etymology. The species name *brevispinus* is derived from Latin: *brevis*, "short", and *spina*, "spine." It refers to the characteristic short propodeal apophysis. The name is an adjective and is in the masculine form to agree with the masculine gender of the genus *Heinrichiellus*.

Comparative diagnosis. The new species is morphologically similar to *H. vedani* sp. nov. In addition to the characters used in the key, *H. brevispinus* sp. nov. can be distinguished from *H. vedani* sp. nov. by the following characters: first flagellomere 6.7 × as long as apical width (5.5 × in *H. vedani* sp. nov.), second tergite 2.1 × as long as wide anteriorly (1.8 × in *H. vedani* sp. nov.) and fifth tergite yellowish (with brownish patch in *H. vedani* sp. nov.).

Heinrichiellus natgeo Ranjith & Broad, sp. nov.

https://zoobank.org/AE976E12-09E3-4745-9027-F255B74C94CF

Material examined. ***Holotype*:** • female, India: Arunachal Pradesh, Yingku, 5.v.2022, Yellow pan trap, coll. Ranjith A.P. (ZSIK: ZSI/WGRC/I.R.-INV.28943). ***Paratype*** • 1 male with same data as holotype (ZSIK: ZSI/WGRC/I.R.-INV.28944) (with following DNA data: sample ID CCDB-44298-H01, BOLD Process ID BBTH5022-22; GenBank accessions: COI PQ858774, 16S PQ873015, 28S PQ873014).

Holotype. ♀, body length 10.7 mm, fore wing length 7.7 mm.

Description of female. ***Head.*** Head 1.2 × as wide as high in anterior view, 1.5 × as wide as long in dorsal view, minutely punctate (Fig. 5B, C); ocellar-ocular length (OOL)/postero-ocellar length (POL) = 1.0. Frons slightly convex above each antennal socket (Fig. 5C); frons granulate with small and distinct tubercle between antennal sockets

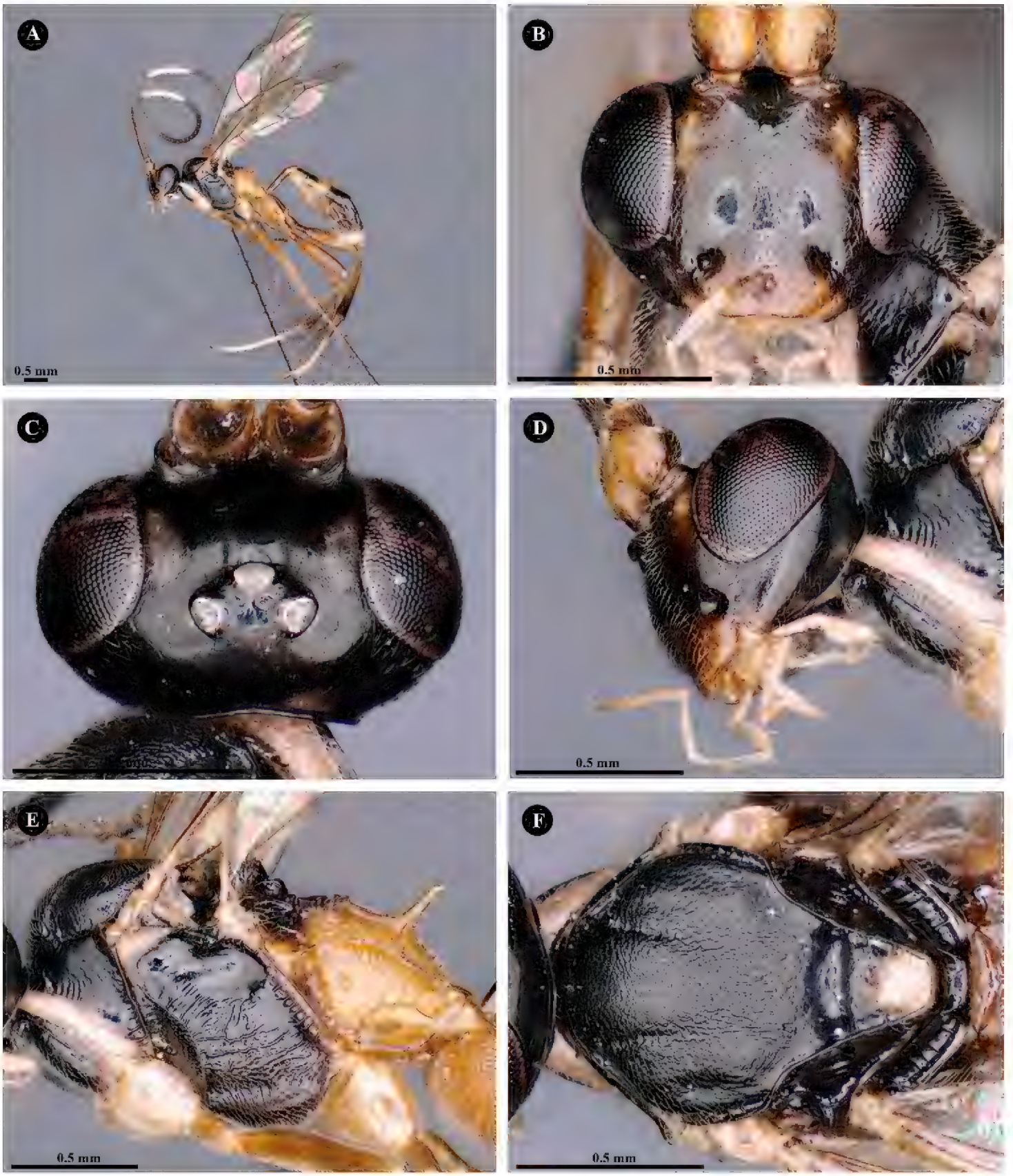

Figure 5. *Heinrichiellus natgeo* Ranjith & Broad, sp. nov., holotype, female **A** habitus, lateral view **B** head, anterior view **C** head, dorsal view **D** head, ventro-lateral view **E** mesosoma, lateral view **F** mesosoma, dorsal view.

(Fig. 5C); antennal sockets large and protruding anteriorly in dorsal view (Fig. 5C); face 1.4 × as wide as high, smooth, irregularly sculptured below antennal socket (Fig. 5B); inner margins of compound eyes slightly diverging ventrally (Fig. 5B); clypeus strongly convex and transverse, 1.6 × as wide as high, with medially concave apical margin (Fig. 5B); anterior tentorial pits large (Fig. 5B); labrum very wide, 0.6 × as wide as clypeus, with straight apical margin, protruding from under clypeus (Fig. 5B). Mandible

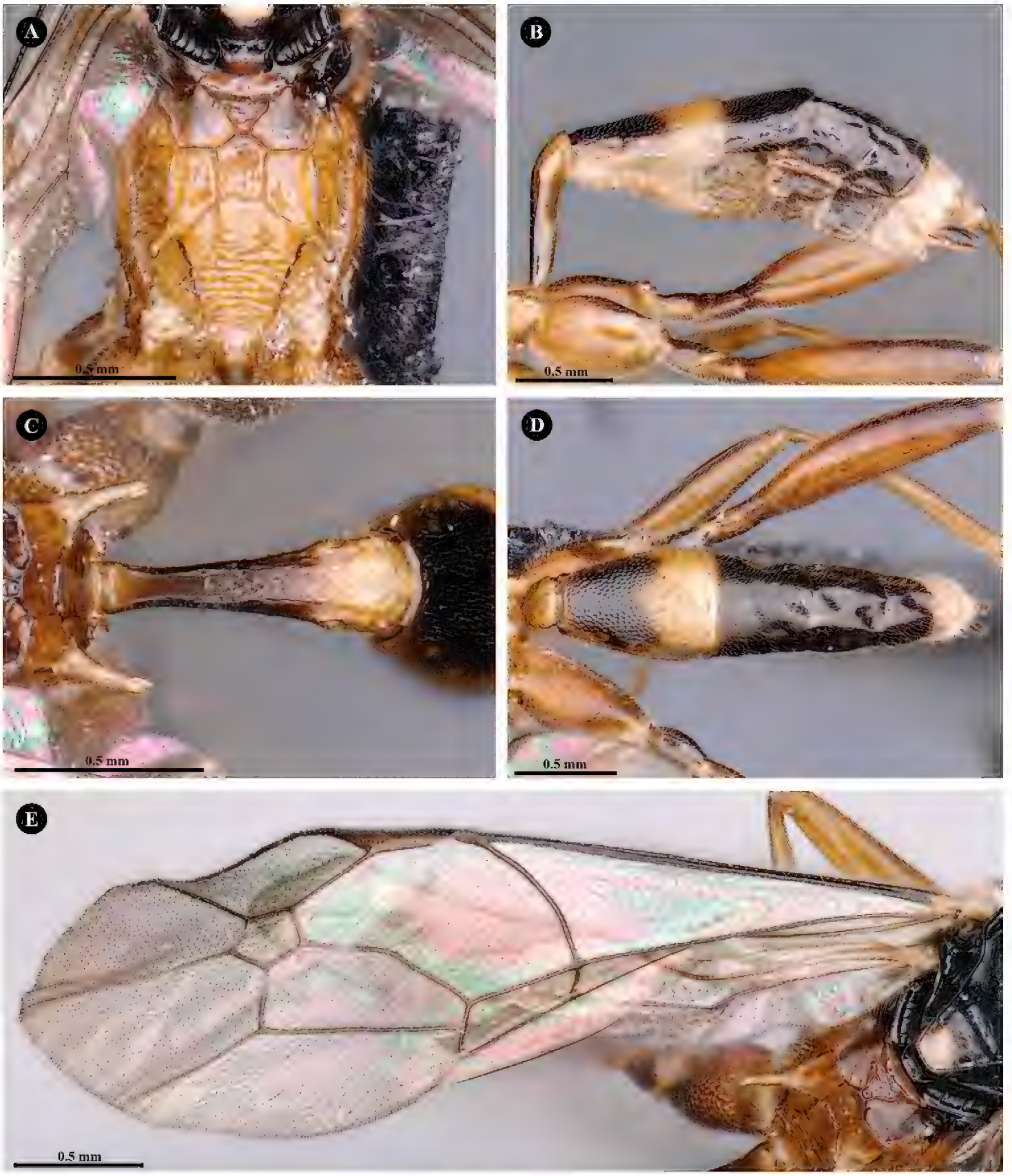

Figure 6. *Heinrichiellus natgeo* Ranjith & Broad, sp. nov., holotype, female **A** propodeum, dorsal view **B** metasoma, lateral view **C** first metasomal tergite, dorsal view **D** metasomal tergite 2–6, dorsal view **E** fore wing.

slender, 2.8 × as long as wide at base, gradually narrowed from base to apex, with indistinct lower tooth (Fig. 5B, D). Malar space granulate, 3.2 × as wide as base of mandible (Fig. 5D). Occipital carina complete, joining hypostomal carina above base of mandible (Fig. 5D); dorso-median part of occipital carina evenly arched (Fig. 5C). Maxillary palp long, reaching epicnemial carina (Fig. 5D); fifth segment 5.0 × as long as mandible base. Dorsal length of eye 1.7 × as long as temple. Antenna with 36 antennomeres. Flagellum

bristle-shaped, very long and slender (Fig. 5A); apical flagellomere conical; first flagellomere 6.2 × as long as apical width and 1.8 × as long as second one.

Mesosoma. Mesosoma 1.6 × as long as high. Collar of pronotum long (Fig. 5D–F). Pronotum strigose on coriaceous surface laterally (Fig. 5D, E). Mesoscutum strongly convex (Fig. 5E), with notaulus reaching middle of mesoscutum (Fig. 5F); surface of mesoscutum granulate with scattered punctures except longitudinally strigose postero-median portion (Fig. 5F). Epicnemial carina complete (Fig. 5E); subtegular ridge sharp (Fig. 5E); impression below speculum weak (Fig. 5E); sternaulus distinct, crenulate, sharp, almost reaching base of mid coxa (Fig. 5E); posterior transverse carina of mesosternum absent; surface of mesopleuron obliquely strigose, smooth anteriorly, speculum slightly polished (Fig. 5E). Scutellum highly elevated above metanotum (Fig. 5E), with crenulate lateral carina reaching apex and dorsal surface almost flat (Fig. 5F); hind margin of metanotum with a triangular projection on each side of metanotum (Figs 5F, 6A). Juxtacoxal carina distinct, complete (Fig. 5E). Propodeum in profile with triangular area basalis flat and evenly slanted from base of area superomedia (Fig. 5E); regular carinae of propodeum complete (Fig. 6A); area superomedia hexagonal, 1.4 × as long as wide (Fig. 6A); apex of area dentipara with very strongly developed, long and sharp apophysis, almost perpendicular to surface of propodeum, apophysis almost straight (Fig. 6A); surface of propodeum smooth (Fig. 6A); area petiolaris indistinct laterally, transversely strigose (Fig. 6A). Propodeal spiracle 1.4 × as long as wide.

Legs. Legs very slender and long (Fig. 5A); all legs longer than fore wing. Hind femur and tibia 4.5, 7.0 × as long as maximum width respectively; ratio of length of tibiae fore:mid:hind = 1.0:1.1:1.6.

Wings. Fore wing 5.9 mm long; areolet 1.5 × as wide as long, 1.5 × as high as 3rs-m, 0.9 × as high as 2m-cu, pentagonal and sides nearly parallel, slightly narrowing anteriorly (Fig. 6E); 1cu-a opposite M&RS (Fig. 6E); ramulus absent (Fig. 6E). Hind wing with cu-a one-fourth as long as first abscissa of CU.

Metasoma. Metasoma mostly coriaceous (Fig. 6B–D). First tergite in profile almost straight, slightly bent downward at base of postpetiole (Fig. 6B), smooth anteriorly, irregularly sculptured between latero-median carinae; in dorsal view 5.0 × as long as wide at base (Fig. 6C); petiole very long, rounded in cross-section, of approximately equal width and height (Fig. 6B, C); in dorsal view petiole slightly broadened posteriorly; latero-median carina present only on anterior portion of postpetiole (Fig. 6C). Second tergite in dorsal view 2.6 × as long as wide anteriorly, distinctly punctate (Fig. 6D). Gastrocoelus slightly impressed, in form of longitudinal groove (Fig. 6D). Thyridium oval, distant from base of second tergite by 0.3 × its length (Fig. 6D). Tergites 3–6 smooth with laterotergites separated by distinct creases (Fig. 6B). Sternites 2–5 laterally sclerotized and middle part not sclerotized (Fig. 6B). Hypopygium with apical margin rounded and longitudinally folded in middle. Ovipositor sheath with apex pointed, protruding beyond apex of metasoma (Fig. 6B).

Colour. Body black except following: clypeus apically, maxillary and labial palps, face antero-laterally, scape and pedicel, flagellomeres 7–11, frons laterally, pronotum antero-laterally, mesopleuron anteriorly, scutellum posterior half, propodeum,

metapleuron, fore and mid legs except tarsi, hind coxa, femur, tibia proximal half, basitarsus distal half, tarsomeres 2–4, first metasomal tergite posterior 1/3, second metasomal tergite posterior half, metasomal tergites 6–7, ovipositor yellow.

Male. Similar to female except: body length 5.1 mm, white inner orbits and clypeus laterally, apically; dorsal inner orbit patch narrowly separated from wider white line below antennal sockets. T1 and hind coxa (rest of hind legs missing) largely dark brown. Gonostyle narrow, 'finger-like'.

Distribution. Oriental region (India).

Etymology. We dedicate the new species to the National Geographic Society (NGS) for their outstanding support for the Siang Expedition in which specimens of the new species were collected. It's a humble dedication to the society in recognition of their committed support to explore, illuminate and protect the wonders of our world through research. The epithet *natgeo* is treated as a noun in apposition.

Comparative diagnosis. The new species is distinctive and unique as the fore wing areolet is very large, hardly narrowing anteriorly. The propodeal spiracle is also shorter than in other *Heinrichiellus*, 1.4 × as long as wide. Superficially this species resembles *Heinrichiellus brevispinus* sp. nov. but can additionally be separated by the length of the propodeal apophyses and the shape of the area superomedia.

Heinrichiellus vedani Ranjith, sp. nov.

https://zoobank.org/4EF29C01-B910-4922-9707-F66B1603C0D3

Material examined. ***Holotype*:** • female, India: Karnataka, Chamarajanagar, Biligiri Rangaswamy Temple Tiger Reserve, scrub jungle, 12°0141.4'N, 77°0655.1'E, 4.x–17.xi.2005, Malaise trap, coll. D.R. Priyadarsanan (ZSIK: ZSI/WGRC/I.R.-INV.29361). ***Paratypes*:** • 2 females and 2 males with same data as holotype (ZSIK).

Holotype. ♀, body length 6.0 mm, fore wing length 4.5 mm.

Description of female. ***Head.*** Head 1.1 × as wide as high in anterior view, 1.9 × as wide as long in dorsal view (Fig. 7B, C); ocellar-ocular length (OOL)/postero-ocellar length (POL) = 0.7. Frons slightly convex above each antennal socket (Fig. 7C); frons granulate without small and distinct tubercle between antennal sockets (Fig. 7C); antennal sockets large and protruding anteriorly in dorsal view (Fig. 7C); face 1.2 × as wide as high, minutely punctate associated with oblique striations medially forming 'V'-shaped area (Fig. 7B); inner margins of compound eyes slightly diverging ventrally (Fig. 7B); clypeus strongly convex and transverse, 2.2 × as wide as high, with medially concave apical margin (Fig. 7B); anterior tentorial pits large (Fig. 7B); labrum very wide, 0.5 × as wide as clypeus, with straight apical margin, protruding from under clypeus (Fig. 7B). Mandible slender, 2.1 × as long as wide at base, gradually narrowed from base to apex, with indistinct lower tooth (Fig. 7B, F). Malar space granulate, 1.9 × as wide as base of mandible (Fig. 7D, E). Occipital carina complete, joining hypostomal carina above base of mandible (Fig. 5D); dorso-median part of occipital carina evenly arched (Fig. 7C). Maxillary palp long, reaching epicnemial carina; fifth segment 4.0 × as long

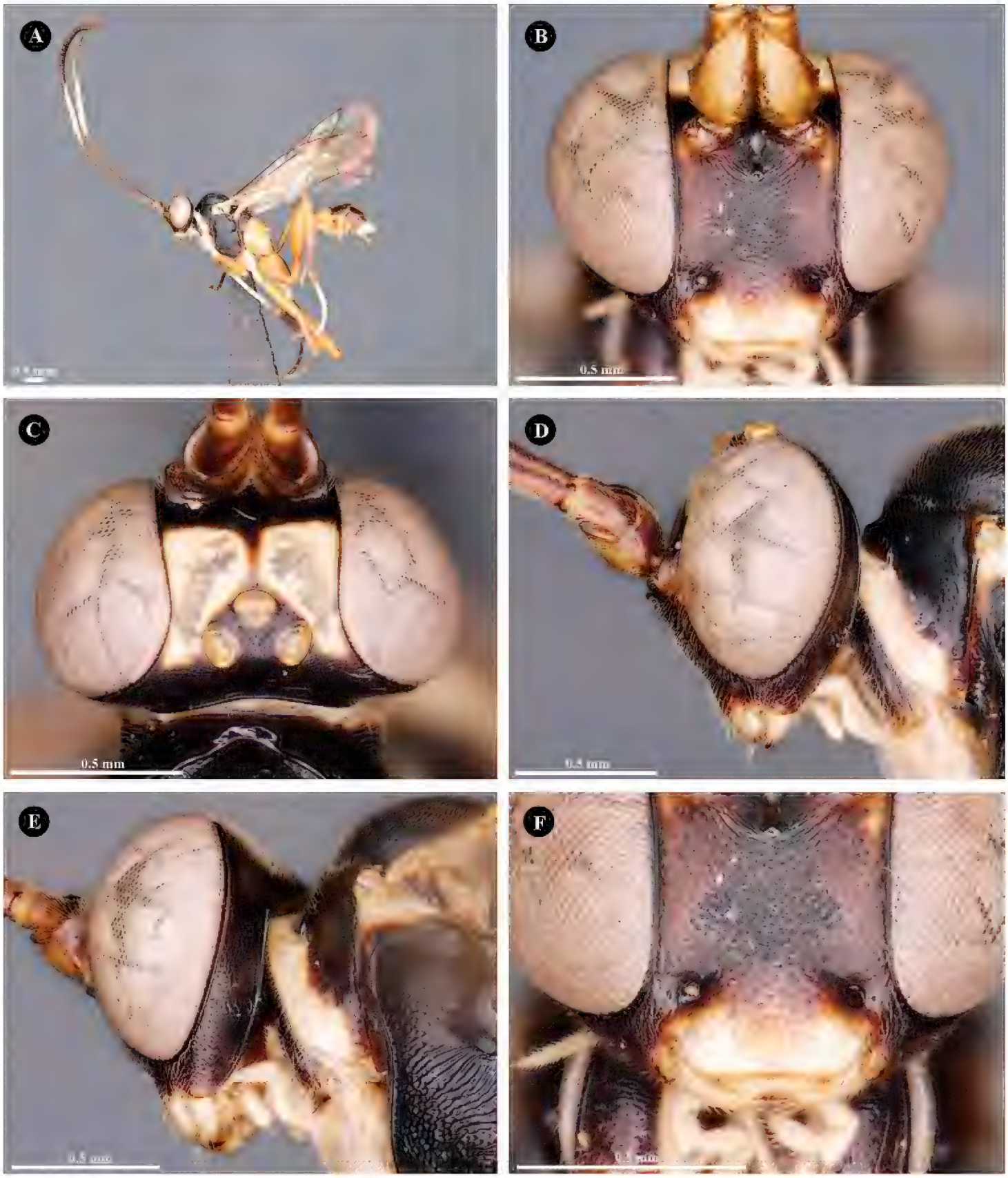

Figure 7. *Heinrichiellus vedani* Ranjith, sp. nov., holotype, female **A** habitus, lateral view **B** head, anterior view **C** head, dorsal view **D** head, lateral view **E** head, ventro-lateral view **F** clypeus and mandible, anterior view.

as mandible base. Dorsal length of eye 3.7 × as long as temple. Antenna with 36 antennomeres. Flagellum bristle-shaped, very long and slender (Fig. 7A); apical flagellomere conical; first flagellomere 5.5 × as long as apical width and 1.4 × as long as second one.

Mesosoma. Mesosoma 1.6 × as long as high. Collar of pronotum long (Fig. 8A, B). Pronotum indistinctly strigose on smooth surface laterally (Figs 7D, 8A). Mesoscutum strongly convex (Fig. 8A), with notaulus nearly absent, only impressed in the form

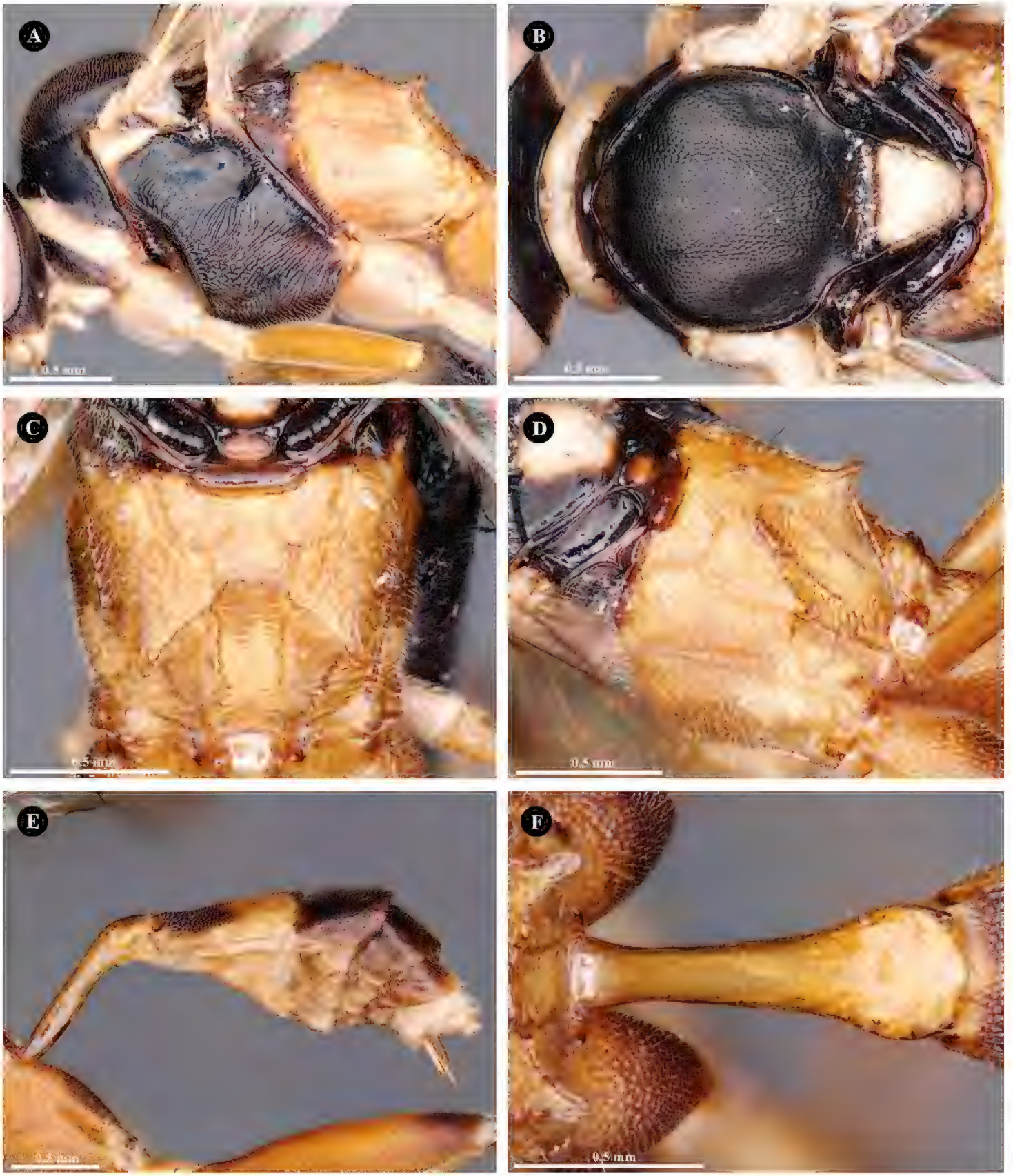

Figure 8. *Heinrichiellus vedani* Ranjith, sp. nov., holotype, female **A** mesosoma, lateral view **B** mesosoma, dorsal view **C** propodeum, dorsal view **D** propodeum, dorso-lateral view **E** metasoma, lateral view **F** first tergite, dorsal view.

of longitudinal strigose sculpture (Fig. 8B); surface of mesoscutum granulate with scattered punctures except longitudinally strigose postero-median portion (Fig. 8B). Epicnemial carina complete (Fig. 8A); subtegular ridge sharp (Fig. 8A); impression below speculum moderately deep (Fig. 8A); sternaulus distinct, crenulate, sharp, almost reaching base of mid coxa (Fig. 8A); posterior transverse carina of mesosternum absent; surface of mesopleuron obliquely strigose, smooth anteriorly, speculum

slightly polished (Fig. 8A). Scutellum highly elevated above metanotum, with crenulate lateral carina reaching apex and dorsal surface almost flat (Fig. 8B); hind margin of metanotum with a triangular projection on each side of metanotum (Fig. 8C, D). Juxtacoxal carina distinct, complete (Fig. 8A). Propodeum in profile with area basalis flat and evenly slanted from base of area superomedia; area basalis not defined by carinae (Fig. 8C); regular carinae of propodeum complete (Fig. 8C, D); area superomedia hexagonal, 0.8 × as long as wide, posterior margin concave (Fig. 8C); apex of area dentipara with strongly developed, moderately long and sharp apophysis, almost perpendicular to surface of propodeum, apophysis almost straight (Fig. 8A); surface of propodeum mostly transversely strigose (Fig. 8C); area petiolaris distinct laterally, transversely strigose (Fig. 8C). Propodeal spiracle 1.5 × as long as wide.

Legs. Legs very slender and long (Fig. 7A); all legs longer than fore wing. Hind femur and tibia 4.0, 7.0 × as long as maximum width respectively; ratio of length of tibiae fore:mid:hind = 1.0:1.3:2.7.

Wings. Fore wing 4.5 mm long; areolet 1.3 × as wide as long, 1.4 × as high as 3rs-m, 0.7 × as high as 2m-cu, pentagonal and sides narrowing anteriorly (Fig. 9B); 1cu-a opposite M&RS (Fig. 9B); ramulus absent (Fig. 9B). Hind wing with cu-a one-fourth as long as first abscissa of CU.

Metasoma. Metasoma mostly coriaceous (Figs 8E, F, 9A). First tergite in profile almost straight, slightly bent downward at base of postpetiole (Fig. 8E), smooth anteriorly, irregularly sculptured between latero-median carinae, coriaceous posteriorly; in dorsal view 4.5 × as long as wide at base (Fig. 8F); petiole very long, rounded in cross-section, of approximately equal width and height (Fig. 8E, F); in dorsal view petiole distinctly broadened posteriorly; latero-median carina present only on anterior portion of postpetiole (Fig. 8F). Second tergite in dorsal view 1.8 × as long as wide anteriorly, distinctly rugose-punctate (Fig. 9A). Gastrocoelus slightly impressed, in form of longitudinal groove (Fig. 9A). Thyridium oval, distant from base of second tergite by 0.3 × its length (Fig. 9A). Tergites 3–4 minutely punctate, 4–6 smooth with laterotergites separated by distinct creases (Fig. 9A). Sternites 2–5 laterally sclerotized and middle part not sclerotized (Fig. 8E). Hypopygium with apical margin rounded and longitudinally folded in middle. Ovipositor sheath with apex blunt, protruding beyond apex of metasoma (Fig. 8E).

Colour. Body mostly yellow except for following: flagellomeres 2–6 (proximal half), 14–34, face except laterally, clypeus except basal half, frons anteriorly, ocellar area, vertex and occiput, temple, pronotum except laterally, propleuron, mesoscutum, metanotum, mesopleuron, wing venation, anterior half of second metasomal tergite, metasomal tergites 3–4, metasomal tergite 5 anteriorly dark brown to black, telotarsi, mid tarsus, hind femur and tibia distally, ovipositor sheath brown.

Male. Similar to female except: body length 6.9 mm, antenna with 35 antennomeres, face yellow except medio-longitudinally, clypeus completely yellow, frons medially black, mesopleuron with yellow patch posteriorly, area superomedia wider than long, second metasomal tergite completely yellow, flagellomeres 1–11, 15–33, brown, 12–14 yellow. Gonostyle narrow, 'finger-like'.

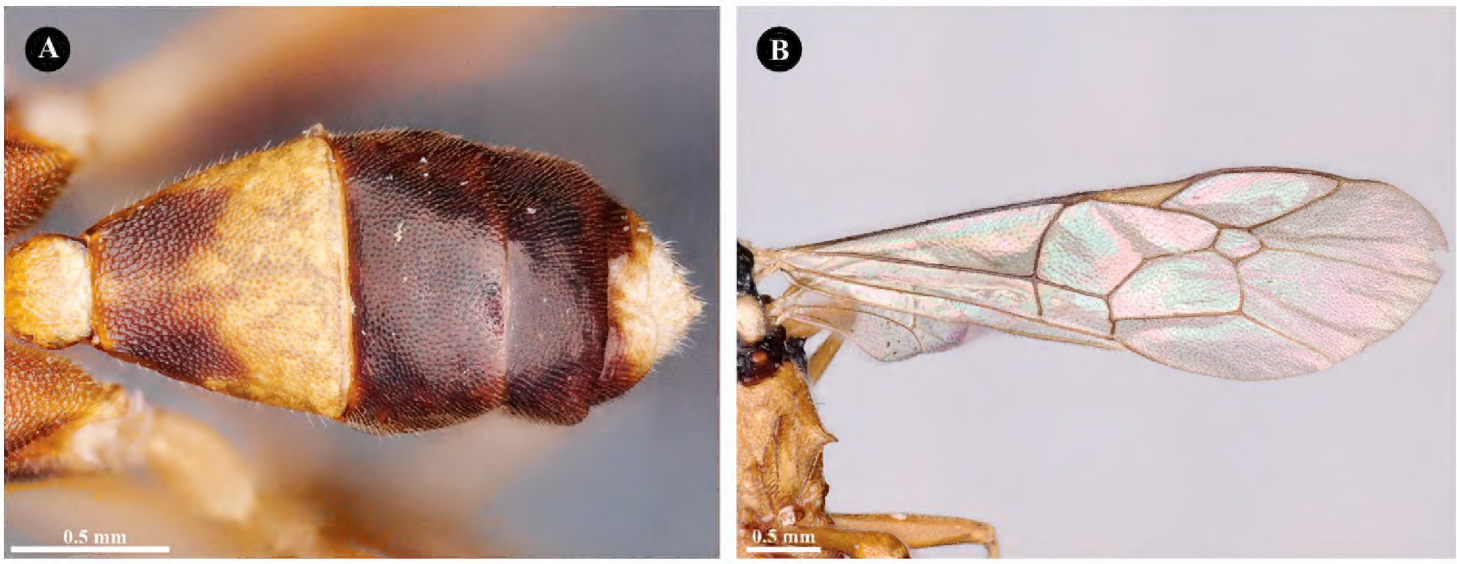

Figure 9. *Heinrichiellus vedani* Ranjith, sp. nov., holotype, female **A** metasomal tergites 2–5, dorsal view **B** fore wing.

Variation. One female paratype with wider longitudinal yellowish patch on face laterally and clypeus completely yellow.

Distribution. Oriental region (India).

Etymology. APR dedicates this species in honor of Vedan (Hirandas Murali), a contemporary singer from Kerala whose work transcends musical boundaries and resonates across political and cultural divides. Vedan's music is noted for its capacity to inspire reflection, unity, and dialogue among individuals of differing political and cultural views, offering a sonic space where contrasting ideologies can intersect through shared emotional and aesthetic experience. This name pays tribute to the artist's unique role in fostering connection and empathy in an increasingly polarized world.

Comparative diagnosis. The new species is morphologically closer to *H. brevispinus* sp. nov., based on the shape of the area superomedia and colour of the frons. Apart from the differences cited in the identification key, *H. vedani* sp. nov. differs from *H. brevispinus* sp. nov. by the following: clypeus yellow in ventral half (dark brown in *H. brevispinus* sp. nov.), malar space 1.9 × as long as basal width of mandible (1.1 × in *H. brevispinus* sp. nov.) and first tergite 4.5 × as long as anterior width (5.1 × in *H. brevispinus* sp. nov.).

Acknowledgements

APR was supported by the Rachadaphiseksomphot Fund, Chulalongkorn University. APR is thankful to the all members of the Siang Expedition 2022 for their immense support and encouragement throughout the period. Sampling in Arunachal Pradesh was funded by a grant from the National Geographic Society, Felis Creations, and supported by the Arunachal Pradesh Forest Department. We sincerely acknowledge the support of Shri Ajai Saxena IFS, retired HoFF and PCCF Arunachal Pradesh for encouraging this expedition and providing the necessary permits. We thank Isuzu

Motors-India, Oken Tayeng at Abor Country Travels, and Kuhl for providing help in very valuable ways. APR is thankful to NGS Expedition and Dr Priyadarsanan Dharma Rajan of Insect Biosystematics and Conservation Laboratory, Ashoka Trust for Research in Ecology and the Environment [ATREE] for sharing the specimens. The authors are thankful to Prof. Michael Sharkey and Dr Stephanie Clutts for access to their Malaise trap materials from the TIGER project (Thailand). APR is thankful to Dr Bijoy C. (Christ College, Kerala, India) for lab facilities. We are grateful to Prof. Paul D.N. Hebert and the Centre for Biodiversity Genomics, Canada for sequencing support. This research is funded by Thailand Science Research and Innovation Fund Chulalongkorn University (BCG_FF_68_178_2300_039) and RSPG Chula to BAB. We sincerely thank the Editor and the reviewers for their valuable comments and suggestions on the earlier version of the manuscript.

References

Belshaw R, Quicke DLJ (1997) A molecular phylogeny of the Aphidiinae (Hymenoptera: Braconidae). Molecular Phylogenetics & Evolution 7: 281–293. https://doi.org/10.1006/mpev.1996.0400

Broad GR, Shaw MR, Fitton MG (2018) Ichneumonid wasps (Hymenoptera: Ichneumonidae): their classification and biology. Handbooks for the Identification of British Insects 7(12): 1–418. https://doi.org/10.1079/9781800625471.0000

de Waard JR, Ivanova NV, Hajibabaei M, Hebert PDN (2008) Assembling DNA barcodes: analytical protocols. In: Martin CC (Ed.) Methods in molecular biology: environmental genetics. Totowa, NJ: Humana Press, 275–283. https://doi.org/10.1007/978-1-59745-548-0_15

Faircloth BC (2016) PHYLUCE is a software package for the analysis of conserved genomic loci. Bioinformatics 32: 786–788. https://doi.org/10.1093/bioinformatics/btv646

Guindon S, Dufayard J-F, Lefort V, Anisimova M, Hordijk W, Gascuel O (2010) New algorithms and methods to estimate maximum-likelihood phylogenies: Assessing the performance of PhyML 3.0. Systematic Biology 59: 307–321. https://doi.org/10.1093/sysbio/syq010

Hajibabaei M, de Waard JR, Ivanova NV, Ratnasingham S, Dooh RT, Kirk SL, Mackie PM, Hebert PDN (2005) Critical factors for assembling a high volume of DNA barcodes. Philosophical Transactions of the Royal Society of London, B Biological Sciences 360: 1959–1967. https://doi.org/10.1098/rstb.2005.1727

Harris RA (1979) A glossary of surface sculpturing. California Department of Food and Agriculture, Bureau of Entomology, Occasional Paper, No. 28: 1–31.

Hebert PDN, Cywinska A, Ball SL, de Waard JR (2003) Biological identification through DNA barcodes. Proceedings of the Royal Society of London Series A: Biological Sciences 270: 96–99. https://doi.org/10.1098/rspb.2002.2218

Hebert PDN, Penton EH, Burns JM, Janzen DH, Hallwachs W (2004) Ten species in one: DNA barcoding reveals cryptic species in the neotropical skipper butterfly *Astraptes fulgerator*. Proceedings of the National Academy of Sciences of the United States of America 101: 14812–14817. https://doi.org/10.1073/pnas.0406166101

Hoang DT, Chernomor O, von Haeseler A, Minh BQ, Vinh LS (2018) UFBoot2: Improving the ultrafast bootstrap approximation. Molecular Biology and Evolution 35: 518–522. https://doi.org/10.1093/molbev/msx281

Ivanova NV, de Waard JR, Hebert PDN (2006) An inexpensive, automation-friendly protocol for recovering high-quality DNA. Molecular Ecology Notes 6: 998–1002. https://doi.org/10.1111/j.1471-8286.2006.01428.x

Kalyaanamoorthy S, Minh BQ, Wong TKF, von Haeseler A, Jermiin LS (2017) ModelFinder: Fast model selection for accurate phylogenetic estimates. Nature Methods 14: 587–589. https://doi.org/10.1038/nmeth.4285

Katoh K, Misawa K, Kuma K, Miyata T (2002) MAFFT: A novel method for rapid multiple sequence alignment based on fast Fourier transform. Nucleic Acids Research 30: 3059–3066. https://doi.org/10.1093/nar/gkf436

Kikuchi N, Konishi K (2015) Discovery of a new species belonging to the genus *Heinrichiellus* Tereshkin (Ichneumonidae, Ichneumoninae, Platylabini). Journal of Hymenoptera Research 45: 31–40. https://doi.org/10.3897/JHR.45.5301

Magnacca KN, Brown MJ (2010) Mitochondrial heteroplasmy and DNA barcoding in Hawaiian *Hylaeus* (*Nesoprosopis*) bees (Hymenoptera: Colletidae). BMC Evolutionary Biology 10: 174. https://doi.org/10.1186/1471-2148-10-174

Nguyen L-T, Schmidt HA, von Haeseler A, Minh BQ (2015) IQ-TREE: A fast and effective stochastic algorithm for estimating maximum likelihood phylogenies. Molecular Biology and Evolution 32: 268–274. https://doi.org/10.1093/molbev/msu300

Park DS, Suh SJ, Oh HW, Hebert PDN (2010) Recovery of the mitochondrial COI barcode region in diverse Hexapoda through tRNA-based primers. BMC Genomics 11: 1–7. https://doi.org/10.1186/1471-2164-11-423

Purvis A, Garland T (1993) Polytomies in comparative analyses of continuous characters. Systematic Biology 42: 569–575. https://doi.org/10.2307/2992489

Quicke DLJ, Belokobylskij SA, Braet Y, Hebert PDN, van Achterberg C, Prosser SWJ, Austin AD, Fagan-Jeffries EP, Ward DF, Shaw MR, Butcher BA (2020) Phylogenetic reassignment of basal cyclostome braconid parasitoid wasps (Hymenoptera) with description of a new, enigmatic Afrotropical tribe with a highly anomalous 28S D2 secondary structure. Zoological Journal of the Linnean Society 190: 1002–1019. https://doi.org/10.1093/zoolinnean/zlaa037

Quicke DLJ, Jasso-Martínez JM, Ranjith AP, Sharkey MJ, Manjunath R, Naik S, Hebert PDN, Priyadarsanan DR, Thurman J, Butcher BA (2023) Phylogeny of the Braconinae (Hymenoptera: Braconidae): A new tribal order! Systematic Entomology 49: 84–109. https://doi.org/10.1111/syen.12608

Santos BF (2017) Phylogeny and reclassification of Cryptini (Hymenoptera, Ichneumonidae, Cryptinae), with implications for ichneumonid higher-level classification. Systematic Entomology 42: 650–676. https://doi.org/10.1111/syen.12238

Santos BF, Wahl DB, Rousse P, Bennett AMR, Kula R, Brady SG (2021) Phylogenomics of Ichneumoninae (Hymenoptera, Ichneumonidae) reveals pervasive morphological convergence and the shortcomings of previous classifications. Systematic Entomology 46: 704–724. https://doi.org/10.1111/syen.12484

Santos BF, Brady SG (2024) Leveraging museum specimens, genomics and legacy datasets to unravel the phylogeny and biogeography of cryptin wasps (Hymenoptera, Ichneumonidae, Cryptini). Zoologica Scripta 53: 338–357. https://doi.org/10.1111/zsc.12639

Tereshkin A (1996) A new Ichneumoninae Stenopneusticae genus, *Heinrichia*, from the Far East (Hymenoptera, Ichneumonidae). Entomofauna 17: 89–96.

Tereshkin A (2000) Description of the males of *Ulesta nigroscutellata* Tereshkin, 1993 and *Rhadinodonta rufidens* (Wesmael, 1844) and a new name for the genus *Heinrichia* Tereshkin, 1996 (Hymenoptera, Ichneumonidae, Ichneumoninae Stenopneusticae). Entomofauna 21: 229–234.

Tereshkin AM (2009) Illustrated key to the tribes of subfamilia Ichneumoninae and genera of the tribe Platylabini of World fauna (Hymenoptera, Ichneumonidae). Linzer biologische Beiträge 41(2): 1317–1608.

Supplementary material 1

Supplementary file S1

Authors: A. P. Ranjith, Gavin R. Broad, Bernardo F. Santos, Buntika A. Butcher

Data type: txt

Explanation note: Matrix used in the phylogenetic analysis: partition file, UCE dataset (identical to that of Santos et al. 2021) and Sanger (COI, 16S and 28S) dataset.

Copyright notice: This dataset is made available under the Open Database License (http://opendatacommons.org/licenses/odbl/1.0/). The Open Database License (ODbL) is a license agreement intended to allow users to freely share, modify, and use this Dataset while maintaining this same freedom for others, provided that the original source and author(s) are credited.

Link: https://doi.org/10.3897/jhr.98.158760.suppl1

Supplementary material 2

Supplementary file S2

Authors: A. P. Ranjith, Gavin R. Broad, Bernardo F. Santos, Buntika A. Butcher

Data type: tre

Explanation note: Output maximum likelihood tree from IQTREE.

Copyright notice: This dataset is made available under the Open Database License (http://opendatacommons.org/licenses/odbl/1.0/). The Open Database License (ODbL) is a license agreement intended to allow users to freely share, modify, and use this Dataset while maintaining this same freedom for others, provided that the original source and author(s) are credited.

Link: https://doi.org/10.3897/jhr.98.158760.suppl2